Identification and Characterization of Fungi Associated with Leaf Spot Disease of Rubber Trees (*Hevea brasiliensis*) in Pahang, Malaysia

Nur Ain Izzati Mohd Zainudin[1,2]*, Nur'ain Azhar[1], Muhamad Najmi Haikal Rosli[1], Nor Aisyah Md Nordin[1]

[1]Department of Biology, Faculty of Science, Universiti Putra Malaysia, 43400, Serdang. Selangor, Malaysia

[2]Institute of Plantation Studies, Universiti Putra Malaysia,43400 Serdang, Selangor, Malaysia

*E-mail: ainizzati@upm.edu.my

Abstract

Rubber trees are important sources of agricultural income as they are utilized for lumber and latex. Like other crops, they are susceptible to numerous fungal pathogens, especially on their leaves, the most important plant part. Therefore, this study was conducted to identify the fungi associated with leaf spot disease on the leaves of rubber trees. This study aimed to characterize fungi associated with diseased rubber leaves and determine the causative agent of leaf spot disease. A total of 20 fungal isolates were obtained and purified from rubber leaves collected during sampling in rubber plantations in Pahang, Malaysia. All the isolated fungi were identified as *Colletotrichum siamense* (2 isolates), *Diaporthe* sp. (5 isolates), *Lasiodiplodia pseudotheobromae* (1 isolate), *L. theobromae* (7 isolates) and *Neoscytalidium* sp. (5 isolates). Based on a pathogenicity test, it was found that nine isolates were pathogenic towards the leaves of rubber, which were *L. theobromae*, *L. pseudotheobromae*, and *C. siamense*. The lesions on the leaves displayed chlorosis with varying necrotic lesion sizes after 21 days post-inoculation. The isolates of the species *L. theobromae* were the most prevalent, indicating it is more widespread in the region than other species. The findings present data on the potential pathogen of rubber plants and are important to understand further the potential risks and effects of the pathogen in rubber plantations.

Keywords: Isolate, *Lasiodiplodia theobromae,* lesion, pathogen, spot

Introduction

Rubber trees (*Hevea brasilien-sis* Müll.Arg.) are Malaysia's most important contributors to economic wealth. Around 50.5% of the world's rubber production is contributed by Malaysia (Asia Perspective, 2022). In 2020, the Malaysian rubber sector was estimated to provide RM 52.9 billion to the country's Gross National Income (GNI) (Ali et al., 2021). Rubber is mainly grown for lumber production, with latex as a by-

product. The tree's milky latex could be collected from the tree's inner bark, a major rubber source (Killman & Hong, 2013).

Like any other crop, the rubber tree is also susceptible to various diseases, which highly affect rubber production. According to Mazlan et al. (2019), rubber plants in nurseries and mature plantations are vulnerable to various diseases at many stages of development. *Rigidoporus microporus*, a causal agent of white rot, is a major disease affecting tropical rubber trees and some crops worldwide (Andrew et al., 2021). The fungus *Microcyclus ulei*, which is the primary cause of Southern American leaf blight (Castro-Navarro et al., 2020), irregular defoliation caused by *Phytophthora* species (Churngchow & Rattarasarn, 2000), and powdery mildew caused by *Oidium heveae* (Liyanage et al., 2016) are among the severe diseases of rubber trees.

Since many different fungal genera can cause disease, identifying the underlying pathogen becomes crucial for initiating preventive or therapeutic actions. As a result, reliable fungal pathogen identification is required to select effective disease control methods and enhance disease management. Numerous research and surveys have been done on various fungal pathogens of rubber. However, studies on leaf spot diseases in these plants still need to be expanded as many current studies focus on diseases of the bark and roots of the plant rather than on the leaf.

Leaf spot disease is a disease often overlooked. Hence, it is important to understand how this disease greatly affects rubber. Leaf spot diseases significantly reduce the surface area available on leaves to conduct photosynthesis, which in turn causes reductions in growth and production of yield. This study is conducted mainly to add to and improve current existing studies of leaf spot

diseases of rubber trees. This research hopes to provide a new fungal checklist and potential preventative disease control measures to avoid future outbreaks or losses. This study aimed to characterize fungi associated with disease in rubber leaves based on morphological approaches and Internal Transcribed Spacer (ITS) sequence analysis and determine the causative agent of leaf spot disease in Malaysia.

Methods

The research was carried out from January 2022 to March 2023 at the Mycology Research Laboratory and Plant House of the Biology Department, Science Faculty, Universiti Putra Malaysia, Malaysia.

Sampling and Fungal Isolation

Rubber leaves showing leaf spot disease symptoms were collected during sampling in plantations at 3.69322 ºN, 102.46751 ºE in Jengka, Pahang, in March 2022. Twenty leaf samples were collected from three different sites. The collected leaves displayed dark brown, black, or yellowish patches. Some patches were high and gleaming, others had dropped out, leaving irregular holes, and some had light and dark circular halos around them. Several patches grew, eventually combined into huge, angular, or irregular dead lesions. The leaf samples were collected using the convenience sampling method by which the samples were obtained from easy-to-reach areas and access (Stratton, 2021).

The infected leaf samples were observed, and about 3 mm² of the infected lesions were cut using a sterilized scalpel and then placed in 10% Chlorox® for 1 minute, followed by 1% Chlorox® for 30 seconds. It was then transferred into sterile water for 10 seconds and dried on sterile filter paper to blot excess liquid. The tissues were then transferred onto potato dextrose agar (PDA) supplemented with streptomycin (10 ml/L of

medium) and neomycin (6 ml/L of medium). The plates were then incubated at room temperature (Leslie & Summerell, 2008). The developed fungal colonies were then sub-cultured and single-spored onto PDA using a single spore's hyphal tip technique (Cheng et al., 2022).

Morphological Identification

The purified fungal plates were observed based on characteristics such as form, elevation, margin, border, surface, opacity, color, and pigmentation (Watanabe, 2002). Both the upper and bottom parts of the plates were observed and recorded. For micro-morphological characteristics, several media were used to induce fungal sporulation and growth, either potato dextrose agar (PDA), carnation leaf agar (CLA), or Spezieller Nahrstoffarmer agar (SNA) (Fisher et al., 1982; Zainudin et al., 2011).

The microscopic characteristics were observed using the Olympus CX31 compound microscope, and photos were captured using a Dino-Eye Microscope Eyepiece Camera. Characteristics such as the shape and size of conidia, hyphae, fruiting bodies, phialide, chlamydospores, and conidiophores are some of the microscopic characteristics observed for fungal identification (Salvamani & Nawawi, 2014). In the case of fungal isolates that have difficulty forming spores, it was found that using CLA was the most efficient at inducing sporulation (Zheng et al., 2019). The microscopic characteristics of the fungal pathogens were recorded and photographed using a Dino Eye 2.0 eyepiece fixed on a microscope, and the conidia's length and width were measured using the Dino Capture 2.0 software.

Pathogenicity Test

All fungal isolates were used for pathogenicity tests on rubber leaves of healthy 3-month-old rubber seedlings. The variety used was PB 350 clones obtained from a nursery in Kuala Lumpur. All seedlings were laid at Complete Randomized Design (CRD) under Plant House in the Biology Department, Science Faculty, Universiti Putra Malaysia. The seedlings were grown at 12/12 hours of 32 ± 1°C days and 28 ± 2°C nights with humidity of 73.6%.

The leaves were surface-disinfected with 70% alcohol for 30 seconds and air-dried. The leaves were inoculated using the wound-mediated inoculation method by Zhang et al. (2018) with slight modification on rubber. By gently piercing the leaf surface with a sterile needle, about six wound points were introduced to the leaflets: 2 at the apical, two at the middle, and two at the basal part of the leaves. A 5 mm mycelial plug of the fungal isolate was inoculated, mycelial side down, onto the wounded area on the leaf. The plants were placed in the plant house for 21 days and were constantly monitored and observed. After 21 days, the lesion lengths were measured and recorded. The inoculated fungi were reisolated and identified to fulfill Koch's Postulate.

The mean data was derived from the lesion length on the rubber leaves. One-way ANOVA and Tukey's HSD were chosen for the Post Hoc analysis to compare lesion lengths generated by the fungal isolates on the leaf samples. Meanwhile, the IBM SPSS version 26 software for Windows was used for the analysis (Marco, 2004). After that, the pathogenic isolates proceeded to molecular characterisation for species confirmation.

Species Identification of the Pathogenic Isolates Based on Internal Transcribed Spacers Sequence Analysis

The gDNA of the pathogenic fungal cultures were extracted using UltraClean® microbial DNA isolation kit (M0-BIO, Carlsbad, CA, USA) following the manufacturer's instructions. Amplification was done using PCR master mix (Promega, Madison, WI, USA)

according to the manufacturer's directions. Universal primers ITS1 (5'TCCGTAGGTGAACCTGCGG3') and ITS4 (5'TCCTCCGCTTATTGATATGC3') were employed to amplify the ITS rDNA gene from the isolated fungal isolates (White et al., 1990). PCR mixtures were performed using GoTaq® Flexi DNA Polymerase (Promega, USA). The PCR reaction mixtures were prepared: 5 x GoTaq buffer, 10 mM primers ITS1 and ITS4, 2 mM dNTPs, 2 mM MgCl$_2$, 5 u *Taq* Polymerase, 20 ng DNA and ddH$_2$O. PCR amplification reactions started with an initial denaturation at temperatures of 95 °C for 30 seconds and continued with 36 cycles of denaturation at 95°C for 10 seconds, annealing at 59°C for 15 seconds, extension at 72°C for 30 seconds and a single cycle of final extension at 72°C for 5 minutes (Tsui et al., 2011). The PCR reactions were performed using a Professional Standard Thermocycler (Biometra Company, USA).

PCR products were separated by gel electrophoresis using 1% agarose gel and visualized with FloroSafe DNA Stain, supplied by First BASE Laboratories, Singapore. Agarose gel (1.0%) was prepared using 1 x TBE buffer. A 100 bp DNA ladder from Promega®, USA, was utilized as a marker. The gel photos were taken with the DOC PRINT system (Vilber Lourmat, USA). The PCR products were submitted to Apical Scientific Sdn. Bhd. (Selangor, Malaysia) for DNA purification and sequencing. The purified ITS products were sequenced in both directions using an Applied Biosystems 3730xl DNA Analyzer (Thermo Scientific). The ITS gene sequences were compared to GenBank sequences using the Standard Nucleotide BLAST network services for any similarities found in the National Centre for Biotechnology Information (NCBI) database, which is accessible using Molecular Evolutionary Genetics Analysis (MEGA) software analysis version 11.0 (Menlove et al., 2009). To match the acquired sequences to one another and the sequences in GenBank, Clustal W in MEGA software version 11.0 was used (Raja et al., 2017). All sequences were deposited in the GenBank database.

Results

Morphological Characterization of Fungi Isolated from Rubber Leaves

A total of 20 isolates of fungi were isolated from rubber leaves. All isolates were classified into four genera of fungi. Out of 20 isolates, seven isolates were identified as *L. theobromae* (Pat.) Griffon and Maublanc, followed by *Diaporthe* sp. (5 isolates), *Neoscytalidium* sp. (5 isolates), *Colletotrichum* sp. (2 isolates), and *L. pseudotheobromae* (1 isolate).

Lasiodiplodia sp. produced abundant grey-cottony aerial mycelia with a color range of colonies from dark grey to black (Figure 1A-D). Initially, the colony was white to pale grey, but later matured and aged to a dark grey. On the reverse plate, the colony pigmentation was dark grey to black. The *L. theobromae* paraphyses were cylindrical, septate, and hyaline (Figure 1E). The conidia of *L. theobromae* were cylindrical with sub-ovoid shapes, tapering bases, and rounded apexes (Figure 1F-J). Conidia were formed on leaf substrates cultured on water agar. Conidia of *L. theobromae* ranged in size from 10.16-14.23 μm in diameter by 16.73-24.01 μm in height, with initial hyaline, thin-walled, aseptate, and granular cell characteristics. As for *L. pseudotheobromae*, it has a larger conidia size as compared to *L. theobromae*, in which the average conidia size is measured from 26.78-27.03 μm × 13.97-15.71 μm.
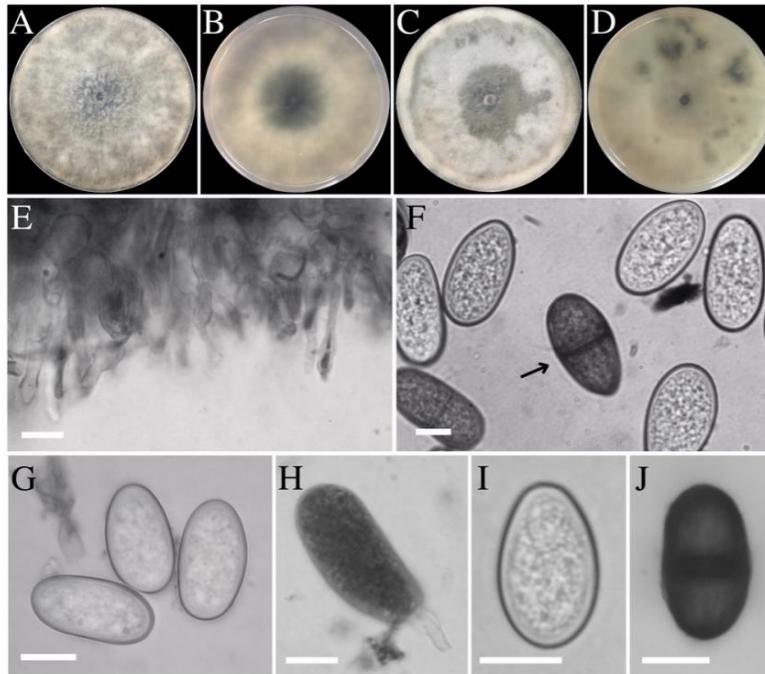
Figure 1. Morphological characteristics of *Lasiodiplodia* sp. (A) *L. theobromae* colony with grey cottony aerial mycelium on PDA. (B) Black to grey pigmentation on the reverse plate of PDA. (C) *L. pseudotheobromae* colony with grey to white cottony aerial mycelium on PDA. (D) Grey pigmentation on the reverse plate of PDA. (E) Conidiogenous cells and septate paraphyses. (F-G) Clusters of conidia (arrow showing matured conidia). (H) Conidium attached to conidiogenous cell (I) Hyaline immature conidia. (J) Mature conidia with middle septum and visible longitudinal striation. Bars: 10 μm

Two isolates of *C. siamense* were obtained from the leaves of a rubber plant. This species' colonies were white cottony with raised elevation and filiform margin. As for the reverse plate, it had a light grey pigmentation (Figure 2A-B). As the isolates aged, numerous little acervuli with orange conidial ooze covered the colony's surface. Chlamydospores were not visible. As for the conidia, they were fusoid-oblong shaped and had no septa. The sizes ranged about 12.01-14.90 μm × 3.84-4.75 μm. There was also the presence of hyaline, cylindrical to ampulliform conidiogenous cells (Figure 2C-G).

Diaporthe sp. colony features ranged from a white, grey to brown feathery surface. Some isolates were also seen to have a grey cottony surface. After two to three weeks, dark-coloured stromata were seen on the agar; some matured to produce pycnidial conidiomata. At the reverse plate, the isolates displayed buff to creamy pigmentation (Figure 3A-D). Swollen hyaline and septate hyphae were also recorded (Figure 3E-F). *Diaporthe* sp. is known to have three types of conidia: alpha, beta, and gamma conidia. However, the gamma conidia were not seen here. The alpha conidia were biguttulate, hyaline, and aseptate. The conidia shapes were fusoid-cylindrical, with sizes ranging from 5.11-7.78 μm × 2.08-2.90 μm. The beta conidia were filiform, one-celled, hyaline, aseptate and had straight or curved ends. The hyphae were observed to be hyaline, septate and swollen (Figure 3G-H).
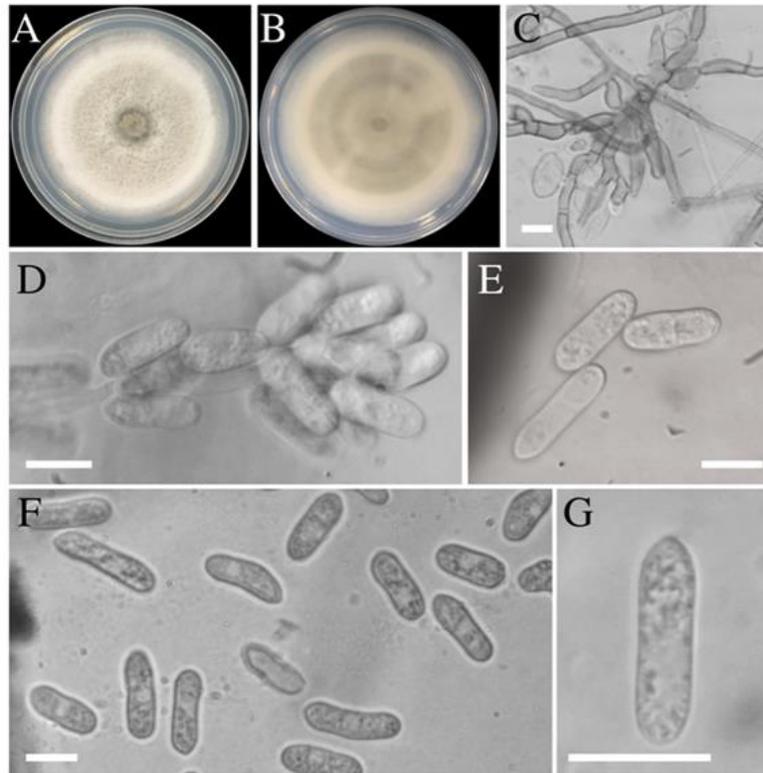
Figure 2. Morphological characteristics of *Colletotrichum siamense.* (A) White cottony colony morphology on PDA. (B) Light grey pigmentation on the reverse plate. (C) Conidiogenous cell. (D-G) Fusoid oblong conidia. Bars: 10 μm
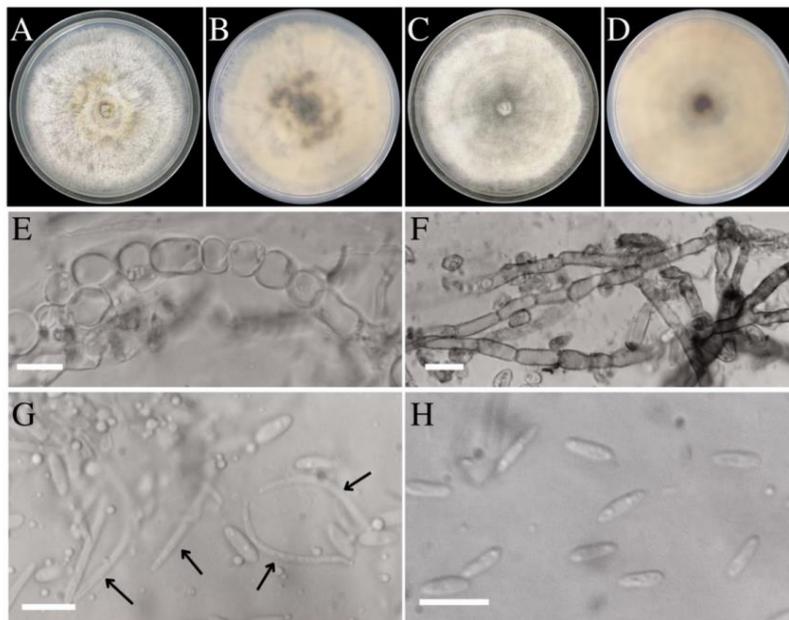

Figure 3. Morphological characteristics of *Diaporthe* sp. (A and D) *Diaporthe* colony with grey and brown feathery aerial mycelium on PDA. (B and D) Creamy pigmentation on the reverse plate of PDA. (E-F) Swollen hyaline, septate hyphae. (G) Filiform beta conidia are shown by arrows. (H) Hyaline, biguttulate alpha conidia. Bars: 10 μm

The colony features of *Neoscytalidium* sp. were observed to be hairy grey to white with flat elevation and filiform margin (Figure 4A). On the reverse plate, a striated brown, black pigmentation can be seen (Figure 4B). The species produced hyaline to brown arthroconidia occurring singly or in arthric chains. The produced conidia have varying shapes and sizes, which were globose, ellipsoid, or cylindrical and ranged in sizes from around 4.18-8.69 µm × 2.54-4.34 µm (Figure 4C-G).

Pathogenicity Test of Leaf Spot Disease

There were 9 isolates analyzed, namely *L. theobromae* isolates C3379R, C3380R, C3381R, C3385R, C3386R, C3387R and C3392R, *L. pseudotheobromae* isolate C3377R and *C. siamense* isolate C3391R, were seen to be significantly different ($p < 0.05$) when compared with the control (Table 1, Figure 5). The mean lesion size ranged from 1.03-6.79 mm. 11 isolates did not display any lesions on the leaves. *L. theobromae* also had the highest number of pathogenic isolates; the biggest lesion size of 6.79 mm was C3385R.
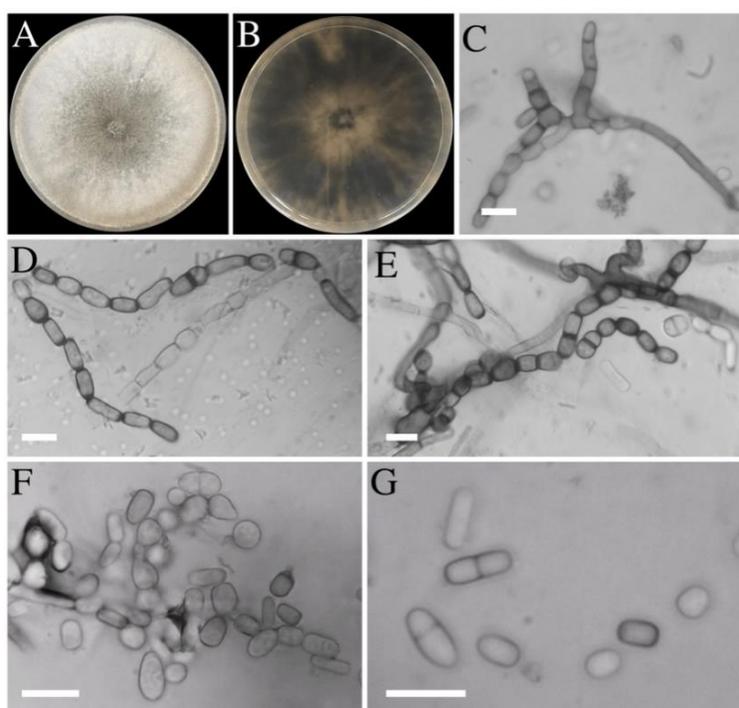

Figure 4. Morphological characteristics of *Neoscytalidium* sp. (A) Hairy grey to white colony morphology on PDA. (B) Brown to black pigmentation on the reverse plate. (C-E) Contiguous arthroconidia (F-G) Various shapes of conidia. Bars: 10 µm.

Table 1. Lesion size on rubber leaves after 21 days of fungal inoculation

No.	Isolate No.	Species	Mean Lesion Size ± SD (mm)	*Pathogenic towards Rubber	Description
	Control	-	0[a]	-	-
1	C3377R	*L. pseudotheobromae*	6.06 ± 1.03[e]	P	Large necrotic lesion with chlorosis
2	C3378R	*Colletotrichum* species	0[a]	N	No visible lesion observed
3	C3379R	*L. theobromae*	1.29 ± 0.63[b]	P	Chlorosis with small necrotic lesion
4	C3380R	*L. theobromae*	1.03 ± 0.25[ab]	P	Chlorosis with small necrotic lesion
5	C3381R	*L. theobromae*	3.93 ± 0.69[d]	P	Chlorosis with small necrotic lesion
6	C3385R	*L. theobromae*	6.79 ± 2.19[e]	P	Large necrotic lesion with chlorosis

No.	Isolate No.	Species	Mean Lesion Size ± SD (mm)	*Pathogenic towards Rubber	Description
7	C3386R	*L. theobromae*	3.96 ± 0.63^d	P	Chlorosis with small necrotic lesion
8	C3387R	*L. theobromae*	5.7 ± 0.82^e	P	Large necrotic lesion with chlorosis
9	C3388R	*Diaporthe* sp.	0^a	N	No visible lesion observed
10	C3389R	*Neoscytalidium* sp.	0^a	N	No visible lesion observed
11	C3391R	*C. siamense*	5.75 ± 1.3^e	P	Chlorosis with small necrotic lesion
12	C3392R	*L. theobromae*	3.5 ± 0.47^d	P	Chlorosis with necrotic lesion
13	C3321R	*Neoscytalidium* sp.	0^a	N	No visible lesion observed
14	C3322R	*Diaporthe* sp.	0^a	N	No visible lesion observed
15	C3323R	*Neoscytalidium* sp.	0^a	N	No visible lesion observed
16	C3324R	*Diaporthe* sp.	0^a	N	No visible lesion observed
17	C3325R	*Diaporthe* sp.	0^a	N	No visible lesion observed
18	C3326R	*Neoscytalidium* sp.	0^a	N	No visible lesion observed
19	C3327R	*Diaporthe* sp.	0^a	N	No visible lesion observed
20	C3328R	*Neoscytalidium* sp.	0^a	N	No visible lesion observed

Different superscript letters in each column indicate that there were significant differences ($p<0.05$). *N= Non-pathogenic, P=Pathogenic
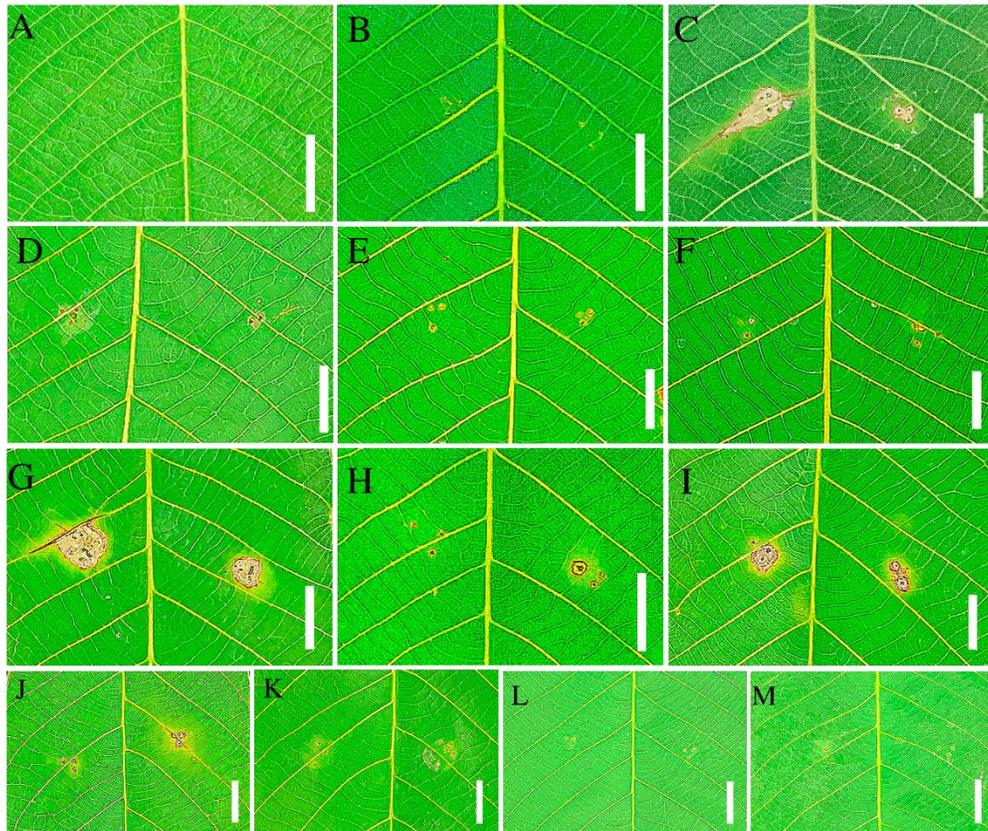

Figure 5. The lesions on rubber leaves after 21 days of fungal inoculation. (A) Non-wounded control, (B) Wounded control, pathogenic isolate from *Lasiodiplodia pseudotheobromae* (C) C3377R pathogenic isolates from *Lasiodiplodia theobromae*; (D) C3379R, (E) C3380R, (F) C3381R, (G) C3385R, (H) C3386R, (I) C3387R, (J) C3392R, pathogenic isolate from *Colletotrichum siamense* (K) C3391R, non-pathogenic isolates; (L) *Diaporthe* sp. isolate C3388R, (M) *Neoscytalidium* sp. isolate C3389R.

Molecular Characterization of Selected Pathogenic Fungal Isolates

The ITS sequences of the pathogenic isolates were amplified, and a comparative analysis of nucleotide sequences was obtained from Genbank. All nine pathogenic isolates were successfully amplified in their ITS regions, with their amplicon size ranging from 537-701 bp (Table 2). The amplified band was used to sequence the region and determine the species. The bands were reproducible and consistently amplified. The nucleotide sequences for all isolates were aligned and edited using MEGA Software and were put into BLAST analysis to find similarities and compared with the established sequences in Genbank (https://blast.ncbi.nlm.nih.gov/Blast.cgi).

Table 2. Species identification of all nine pathogenic isolates associated with rubber leaf samples based on ITS sequence analysis

No.	Isolate no.	Species	Sequence (bp)	ITS accession no.
1	C3377R	*L. pseudotheobromae*	537	OQ132568
2	C3379R	*L. theobromae*	701	OQ132565
3	C3380R	*L. theobromae*	699	OQ132564
4	C3381R	*L. theobromae*	653	OQ132567
5	C3385R	*L. theobromae*	684	OQ132561
6	C3386R	*L. theobromae*	543	OQ132560
7	C3387R	*L. theobromae*	549	OQ132559
8	C3391R	*C. siamense*	555	OQ132557
9	C3392R	*L. theobromae*	560	OQ132556

Discussion

The fungal genus with the highest number of isolates in this study was *Lasiodiplodia* sp., namely *L. theobromae* (Pat.) Griffon and Maublanc. Geographically, it is one of the most widespread species of the Botryosphaeriaceae family that may be found practically anywhere in the world, with a special occurrence in tropical and subtropical areas (Salvatore et al., 2020). It is a non-host-specific plant pathogen or endophyte. Like most species in the Botryosphaeriaceae family, it can be found on various crops and trees (Slippers & Wingfield, 2007). It has been linked to fruit rot, root rot, dieback, and canker diseases. In reality, more than 500 different plant hosts have been connected to *L. theobromae* (Salvatore et al., 2020). One of the distinguishing features of this genus is that the conidia are initially subovoid to ellipsoidal in form and unicellular. Conidia have thick walls, are bi-celled (separated by a septum), and an ellipsoidal form. The immature conidia were subovoid to ellipsoidal in shape and lacked a septum at first. However, as they matured, they developed a single, thick-walled septum (bi-celled) (Hon-ger et al., 2018).

The second-highest number of isolates came from the genus *Diaporthe*. According to Sun et al. (2021), the anamorph of these genus has cylindrical phialides that produce three different types of hyaline, aseptate conidia, called ostiolate conidiomata. The first type is alpha conidia, which comprises hyalines, fusiform, straight, guttulate, or eguttulate, aseptate, and smooth-walled conidia. The second type is beta conidia, consisting of hyaline, filiform, straight or hamate, aseptate, and smooth-walled conidia. The third type is gamma conidia, which have hyaline, multiguttulate, fusiform to subcylindrical, with an acute or rounded

apex and a sometimes-truncate base. Gamma conidia is rarely produced (Guo et al., 2020).

Two isolates of *Colletotrichum* sp. were obtained from the rubber plant leaves. Liu et al. (2022) described that the representative isolates' colonies on PDA are cottony and range from light grey to dark grey. Meanwhile, the aerial mycelium is white to light grey in color and progressively becomes grey. Anggrahini et al. (2020) also stated that the colony is scattered with a few tiny black acervuli or orange conidial masses and that one-celled, cylindrical, hyaline conidia are present.

Based on the pathogenicity test, it was suggested that *L. theobromae* is the most prevalent pathogen causing leaf spot disease in rubber plants. From this study, it accounted for 45% of pathogenic isolates. Numerous cases have been reported worldwide for rubber plants (Cai et al., 2018). Over 500 plant diseases, including fruit rot, root rot, collar rot, stem-end rot, dieback, canker, and leaf necrosis, are caused by the *Lasiodiplodia* sp. (Rusin et al., 2020). Numerous destructive diseases have been linked to *Lasiodiplodia* sp. In addition, they can behave as endophytes or secondary pathogens and develop the ability to cause disease in response to stress (Huda-Shakirah et al., 2022).

There have been numerous reports of *Diaporthe* sp. acting as saprobes, non-pathogenic endophytes, or plant pathogens on a variety of hosts (Gomes et al., 2013). Peruzzo et al. (2019) mentioned that numerous reports and studies of these species were conducted on soybeans. However, no reported cases of this species infecting rubber trees were found (Farr & Rossman, 2023). Reicks (2017) stated that although the plants can become infected during the growing season, this usually happens earlier. Early in the growing season, when the leaves are wet for long periods,

infections are more likely to appear in the field. When it is hot and humid right before maturity, there is a higher likelihood of infection. The disease can enter the plant through tears in the tissue caused by strong winds, hail, and other natural disasters.

Neoscytalidium sp. is mostly known as an opportunistic plant pathogen that causes internal black rot in fruits, as well as pit canker and spots on the stem of plants and fruits (Yi et al., 2015). From the results of the pathogenicity test, it can be seen that two out of four of the isolates caused symptoms of infections on rubber leaves. Pakdaman (2022) mentioned that this species' wide host range reflects its capacity to neutralize a variety of defensive compounds made in various phytochemical factories. Due to its wide host range, including domesticated plants and wild trees, as well as the formation of airborne arthro-conidia, the fungus can be easily spread by wind (Nouri et al., 2018). The fungus is characterized as a soilborne and airborne pathogen that can live in infected debris and damaged trees, although no vector has been identified for the pathogen (Pakdaman, 2022). Until now, there have been no reported cases of this species infecting rubber (Farr & Rossman, 2023).

Colletotrichum siamense is pathogenic to rubber. Although the number of pathogenic isolates is small, preventive measures should be taken to avoid a worse effect on the rate of photosynthesis because the leaves are the affected part. Liu et al. (2018) reported that the prominent issue of rubber plants in Southeast Asia, Sri Lanka, India, and China is *Colletotrichum* leaf disease (CLD) brought on by species of the genus *Colletotrichum*. Liu et al. (2020) described that in severe cases, the concentric rings-shaped anthracnose spots brought on by *Colletotrichum* infection typically develop at the leaf margins but can also arise rarely in

the center of a mature leaf (Saha et al., 2002). These big lesions may combine to form recognizable larger patches of varying sizes. This spot's center is papery and light brown in color. The nearly round, papery lesions with a dark brown center and a yellow halo are another notable leaf spot sign of *Colletotrichum* infection (Du et al., 2021).

Conclusion

Twenty isolates were isolated from rubber leaves, and they were morphologically identified as members of the genus *Lasiodiplodia, Diaporthe, Neoscytalidium*, and *Colletotrichum*. Each genus of the isolated fungi displayed distinctive characteristics in terms of their macroscopic and microscopic characteristics. Out of 20 isolates used, nine isolates (45%) were confirmed to be pathogenic towards rubber trees and caused leaf spot disease. The pathogenic isolates showed significant differences in lesion length compared to the control. *Lasiodiplodia theobromae* showed the biggest lesion size and the highest number of pathogenic isolates.

Acknowledgment

Declaration

Author contribution

Nur Ain Izzati Mohd Zainudin (NAIMZ) is the corresponding author, and Nur'ain Azhar (NA), Muhamad Najmi Haikal Rosli (MNHR) and Nor Aisyah Md Nordin (NAMN) are co-authors. NAIMZ designed the framework of the project, supervised the work, and performed the experiments together with NA. All authors contributed significantly to the conception, design, and/or analysis and interpretation of data. NAIMZ and NA drafted the article, revised it critically for important intellectual content, and contributed to the final approval of the version to be published.

Funding statement

Competing interest

The authors declare no known competing financial interests or personal relationships that could have appeared to influence the work reported in this paper.

References

Andrew B, K Ahmad, SI Ismail, MF Ahmad, OH Ahmed, and MY Wong. 2021. Disease prevalence and molecular characterisation of *Rigidoporus microporus* associated with white root rot disease of rubber tree (*Hevea brasiliensis*) in Malaysia. Journal of Rubber Research 24: 175–186. DOI. 10.1007/s42464-021-00083-x

Anggrahini DS, A Wibowo, and S Subandiyah. 2020. Morphological and molecular identification of *Colletotrichum* spp. associated with chili anthracnose disease in Yogyakarta region. Jurnal Perlindungan Tanaman Indonesia 24(2): 161-174. DOI. 10.22146/jpti.58955.

Asia Perspective. 2022. Rubber manufacturing in southeast asia, an introduction part 2: Vietnam and Malaysia. Retrieved January 4, 2023, from https://www.asiaperspective. com/rubber-manufacturing-vietnam-malaysia/

Cai Z, Y Shi, Y Liu, B Xiong, L Li, F Li, and G Li. 2018. The pathogen causing Lasiodiplodia leaf spot on rubber tree. Journal of Yunnan Agricultural University 33(2): 224-232. DOI. 10.12101/j.issn.1004-390X(n).201709036.

Castro-Navarro OM, DH Riascos-Ortiz, LM Hoyos-Carvajal, and AL Tapiero-Ortiz. 2020. Histological disturbances caused by *Microcyclus ulei* and *Colletotrichum* spp. in rubber trees (*Hevea brasiliensis*). Summa Phytopathologica 46: 105-112. DOI. 10.1590/0100-5405/229849.

Cheng X, L Zhang, J Luo, S Yang, Y Deng, J Li, and C Hou. 2022. Two pathogenic fungi isolated from chalkbrood samples and honey bee viruses they carried. Frontiers in Microbiology   13:   843842.   DOI. 10.3389/fmicb.2022.843842

Churngchow N, and M Rattarasarn. 2000. The elicitin secreted by *Phytophthora palmivora*, a rubber tree pathogen. Phytochemistry 54(1): 33-38. DOI. 10.1016/s0031-9422(99)00530-0.

Marco S, F Calzarano, F Osti, and A Mazzullo. 2004. Pathogenicity of fungi associated with a decay of kiwifruit. Australasian Plant Pathology 33(3): 337-342. DOI. 10.1071/ AP04024.

Du Y, M Wang, L Zou, M Long, Y Yang, Y Zhang, and X Liang. 2021. Quantitative detection and monitoring of *Colletotrichum siamense* in rubber trees using real-time PCR. Plant Disease 105(10):   2861-2866.   DOI. 0.1094/PDIS-10-20-2198-RE .

Farr DF, and AY Rossman. 2023. Fungal databases. U.S. National Fungus Collections, ARS, USDA. Retrieved January 28, 2023, from http://nt.ars-grin.gov/fungaldatabases/,

Fisher NL, LW Burgess, TA Toussoun, and PE Nelson. 1982. Carnation leaves as a substrate and for preserving cultures of *Fusarium* species. Phytopathology 72(1): 151-153. DOI. 10.1094/phyto-72-151.

Gomes RR, C Glienke, SI Videira, L Lombard, JZ Groenewald, and PW Crous. 2013. *Diaporthe*: a genus of endophytic, saprobic and plant pathogenic fungi. Persoonia 31: 1–41. DOI. 10.3767/003158513X666844.

Guo YS, PW Crous, Q Bai, M Fu, MM Yang, XH Wang, and GP Wang. 2020. High diversity of *Diaporthe* species associated with pear shoot canker in China. Persoonia-Molecular Phylogeny and Evolution of Fungi 45(1):

132-162.   DOI.   10.3767/persoonia.2020. 45.05.

Honger JO, SR Coleman, FK Ablormeti, EW Cornelius, E Owusu, and GT Odamtten. 2018. The aetiology, incidence and severity of mango tree decline disease in Ghana. Ghana Journal of Science 58:13-22. https://www.ajol.info/index.php/gjs/article /view/177889.

Huda-Shakirah AR, NMI Mohamed Nor, L Zakaria, YH Leong, and MH Mohd. 2022. *Lasiodiplodia theobromae* as a causal pathogen of leaf blight, stem canker, and pod rot of *Theobroma cacao* in Malaysia. Scientific Reports 12(1): 1-14. DOI. 10.1038/s41598-022-13057-9.

Killman W, and LT Hong. 2001. Rubberwood–the success of an agricultural by-product. World 5: 314.

Leslie JF, and BA Summerell. 2008. *The Fusarium laboratory manual.* John Wiley & Sons.

Liyanage KK, S Khan, PE Mortimer, KD Hyde, J Xu, S Brooks, and Z Ming. 2016. Powdery mildew disease of rubber tree. Forest Pathology   46(2):   90-103.   DOI. 10.1111/efp.12271.

Liu X, B Li, J Cai, X Zheng, Y Feng, G Huang. 2018. *Colletotrichum* species causing anthracnose of rubber trees in China. Scientific Reports 8(1): 1-14. DOI. 10.1038/ s41598-018-28166-7.

Liu X, B Li, Y Yang, J Cai, T Shi, X Zheng, and G Huang. 2020. Pathogenic adaptations revealed by comparative genome analyses of two *Colletotrichum* spp., the causal agent of anthracnose in rubber tree. Frontiers in Microbiology 11: 1484. DOI. 10.3389/ fmicb.2020.01484.

Liu X, Y Li, M Wang, P Cao, H Wang, J Yin. 2022. Stem-end rot caused by *Lasiodiplodia brasiliense* on tobacco in China. Plant Disease 106(12): 3208. DOI. 10.1094/PDIS-03-22-0462-PDN .

Liyanage KK, S Khan, PE Mortimer, KD Hyde, J Xu, S Brooks, Z Ming. 2016. Powdery mildew disease of rubber tree. Forest Pathology 46(2): 90-103.

Mazlan S, NM Jaafar, A Wahab, H Rajandas, D Zulperi. 2019. Major diseases of rubber

(*Hevea brasiliensis*) in Malaysia. Pertanika Journal of Scholarly Research Reviews 5(2): 10-21.

Menlove KJ, M Clement, KA Crandall. 2009. Similarity searching using BLAST. In *Bioinformatics for DNA Sequence Analysis* (pp. 1-22). Humana Press.

Nouri MT, DP Lawrence, MA Yaghmour, TJ Michailides, FP Trouillas. 2018. *Neoscytalidium dimidiatum* causing canker, shoot blight and fruit rot of almond in California. Plant Disease 102(8): 1638-1647. DOI. 10.1094/PDIS-12-17-1967-RE.

Pakdaman BS. 2022. *Neoscytalidium dimidiatum*: an emerging threat in global warmth era. Journal of Biotechnology and Bioresearch 3(4): 1-4. https://crimsonpublishers.com/ jbb/fulltext/JBB.000566.php.

Peruzzo AM, FE Hernández, GR Pratta, LD Ploper, and RN Pioli. 2019. Identification and inheritance of an Rdc gene resistance to soybean stem canker (*Diaporthe phaseolorum var. caulivora*). European Journal of Plant Pathology 154(4): 1179-1184. DOI. 10.37572/EdArt_18122151413.

Reicks S. 2017. *Diaporthe/Phomopsis fungi complex in soybeans* [PDF]. Retrieved from Pioneer. Crop Focus. https://www.pioneer. com/CMRoot/Pioneer/US/Non_Searchable /agronomy/cropfocus_pdf/Diaporthe-Phomopsis-Soybeans.pdf

Rusin C, FR Cavalcanti, PCGD Lima, CMDR Faria, MAK Almança, and RV Botelho. 2020. Control of the fungi *Lasiodiplodia theobromae*, the causal agent of dieback, in cv. syrah grapevines. Acta Scientiarum Agronomy 43: e4478. DOI. 10.4025/ actasciagron.v43i1.44785.

Saha T, A Kumar, M Ravindran, CK Jacob, B Roy, and MA Nazeer. 2002. Identification of *Colletotrichum acutatum* from rubber using random amplified polymorphic DNAs and ribosomal DNA polymer-phisms. Mycological Research 106(2): 215-221. DOI. 10.1017/S095375 6201005342.

Salvamani S, and NM Nawawi. 2014. Macroscopic and microscopic approaches for identification of fungi from plant soil of Cameron Highlands. Bioremediation Science and Technology Research 2(1): 14-18. DOI. 10.54987/bstr.v2i1.68.

Salvatore MM, A Alves, and A Andolfi. 2020. Secondary metabolites of *Lasiodiplodia theobromae:* Distribution, chemical diversity, bioactivity, and implications of their occurrence. Toxins 12(7): 457. DOI. 10.3390/toxins12070457.

Slippers B, and MJ Wingfield. 2007. Botryosphaeriaceae as endophytes and latent pathogens of woody plants: diversity, ecology and impact. Fungal Biology Reviews 21(2-3): 90-106. DOI. 10.1016/j.fbr.2007.06.002.

Stratton SJ. 2021. Population research: convenience sampling strategi-es. Prehospital and Disaster Medicine 36(4): 373-374. DOI. 10.1017/ S1049023X21000649.

Sun W, S Huang, J Xia, X Zhang, and Z Li. 2021. Morphological and molecular identification of *Diaporthe* species in south-western China, with description of eight new species. MycoKeys 77: 65-69. DOI. 10.3897/mycokeys.77.59852.

Tsui CKM, J Woodhall, W Chen, CA Lévesque, A Lau, CD Schoen, C Baschien, MJ Najafzadeh, and GS de Hoog. 2011. Molecular techniques for pathogen identification and fungus detection in the environment. IMA Fungus 2(2): 177–189. DOI. 10.5598/imafungus.2011.02.02.09.

Watanabe T. 2002. Morphology of soil fungi. In Watanabe (Ed.) *Pictorial Atlas of Soil and Seed Fungi: Morphologies of Cultured Fungi and Key to Species, Second Edition* (2nd ed. pp. 39-183). CRC Press.

White TJ, T Bruns, S Lee, and J Taylor. 1990. Amplification and direct sequencing of fungal ribosomal RNA genes for phylogenetics. PCR Protocols: A Guide to Methods and Applications 18(1): 315–322.

Yi RH, JJ Mo, FF Wu, J Chen. 2015. Fruit internal brown rot caused by *Neoscytalidium dimidiatum* on pitahaya in Guangdong province, China. Australasian Plant Disease Notes 10(1): 1-4. DOI. 10.1007/s13314-015-0166-1.

Zainudin NAIM, AR Azmi, MSS Nordahliawate, and J Norazlina. 2011. Contribution to the knowledge of diversity of *Fusarium* associated with maize in Malaysia. Plant Protection Science 47(1): 20-24. DOI. 10.17221/52/2008-PPS.

Zhang M, X Sun, L Cui, Y Yin, X Zhao, S Pan, and W Wang. 2018. The plant infection test: spray and wound-mediated inoculation with the plant pathogen *Magnaporthe grisea*. Journal of Visualized Experiments 138: 57675. DOI. 10.3791/57675.

Zheng Z, YF Wang, H Bai, ZY Li, and ZP Dong. 2019. First report of *Fusarium incarnatum-equiseti* species complex causing ear rot of foxtail millet in Northwest regions of China. New Disease Reports 40: 8-8. DOI. 10.5197/j.2044-0588.2019.040.008.